A017 - Near Field Dynamic, Co-seismic and Post-seismic Deformations Associated with the 2013, M7.8, and 2003, M7.6, South Scotia Ridge Earthquakes Observed with GPS

SMALLEY, R. Jr.[1], BEVIS, M. G.[2], ZAKRAJSEK, A. F.[3], TEFERLE, F. N.[4], DALZIEL, I. W. D.[5], LAWVER, L. A.[5], LARTER, R. D.[6]

1) Center for Earthquake Research and Information, Univ of Memphis, Memphis, TN, USA, rsmalley@memphis.edu
2) School of Earth Sciences, The Ohio State University, Columbus, OH, USA, mbevis@osu.edu
3) Dirección Nacional del Antártico - Instituto Antártico Argentino, Buenos Aires, Argentina, afz@dna.gob.ar
4) Geophysics Laboratory, University of Luxembourg, Luxembourg, Luxembourg, norman.teferle@uni.lu
5) Institute for Geophysics, University of Texas Austin, Austin, TX, USA, ian@utig.ig.utexas.edu
6) British Antarctic Survey, Cambridge, United Kingdom, rdla@bas.ac.uk

Abstract: The South Scotia Ridge (SSR) left-lateral transform/strike-slip (S-S) fault defines the Scotia plate's (SP) southern boundary separating it from the Powell Basin (PB), South Orkney Microcontinent (SOM), and the Weddell Sea sections of the Antarctic plate (AP). The SP developed as a space filling accommodation zone for S. America-Antarctica relative motions, mostly during the last 40 m.y. The SSR also hosts several restraining and releasing bends. The SP, PB and SOM have complex evolution histories including large-scale displacement and stretching of the SOM, as well as other continental fragments within the SP, all of which were incorporated into a background of expanding sea floor spreading geometries.

The SOM defines an ~300 km segment of the SSR opposite a section of the SP that is primarily oceanic crust with a few small, stretched continental fragments. Two large earthquakes, M7.6 and 7.8, with aftershock zones largely confined to the northern SOM boundary, occurred on the SSR in 2003 and 2013. Moment tensor solutions show they occurred on faults dipping ~30 and 45° to the south. The 2013 event was almost pure, left-lateral strike-slip, while the 2003 event was oblique but predominantly strike-slip. This is an unusual combination of fault dip and slip direction for a strike-slip plate boundary. The half duration of both events is also relatively long.

A continuous GPS (CGPS) station on Laurie Island is located immediately west of the rupture zone of the 2003 event and at the approximate center, and close to the surface projection, of the finite fault models for the 2013 earthquake. We present co-seismic static offsets and post-seismic transients for both earthquakes from GPS daily position estimates. In addition, the CGPS station now records at 1 Hz and we present the GPS displacement seismogram for the 2013 event. This record contains a complex signal that includes the passage of the Love and Rayleigh surface waves, with max displacements of ~70 cm, over an ~80 second time interval during which a ~50 cm static offset developed.

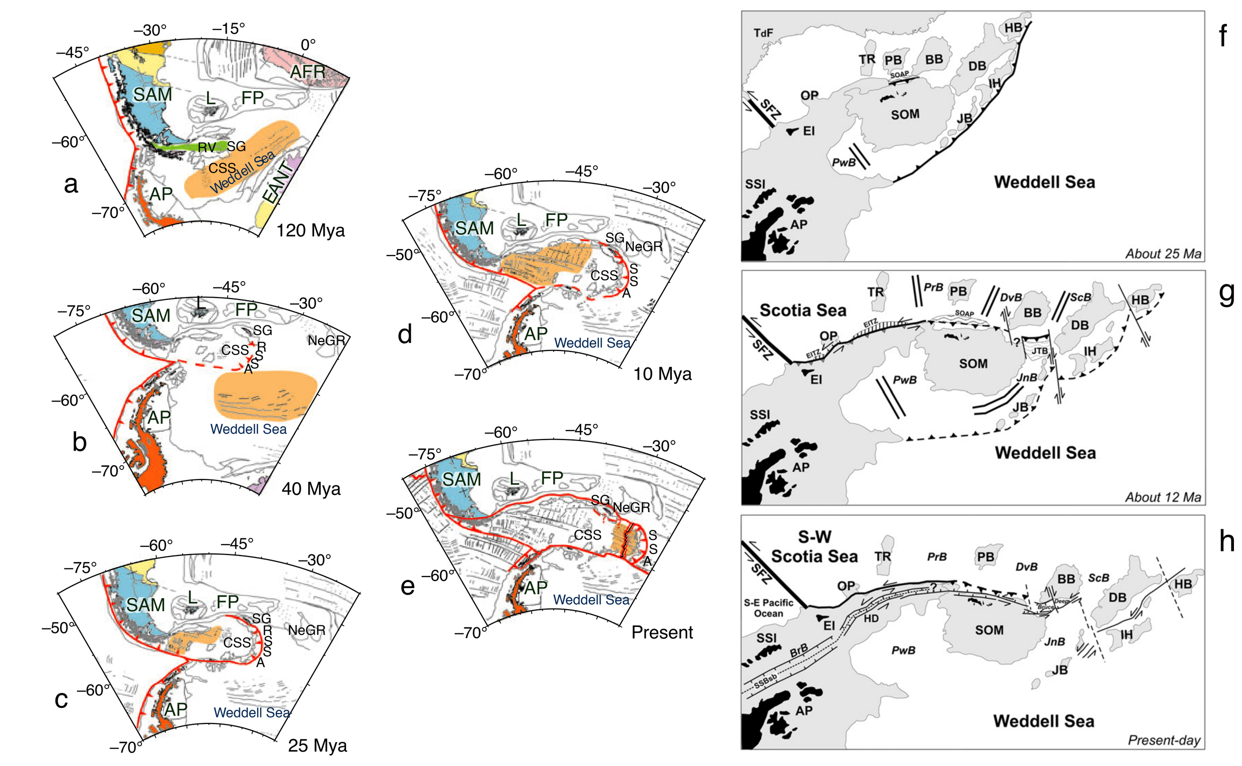

Fig 1. SP tectonic history. Left from Dalziel, et al., 2013, right from Civile, et al., 2012. The modern SP was born ~40 Ma with separation of Antarctica from S. America and opening of Drake Passage. Two significant microcontinents were torn from the northern Antarctic Peninsula (SOM) and southernmost S. America (SG) with opening of the PB and creation of the western SP by the now extinct West Scotia ridge (see Fig 2).

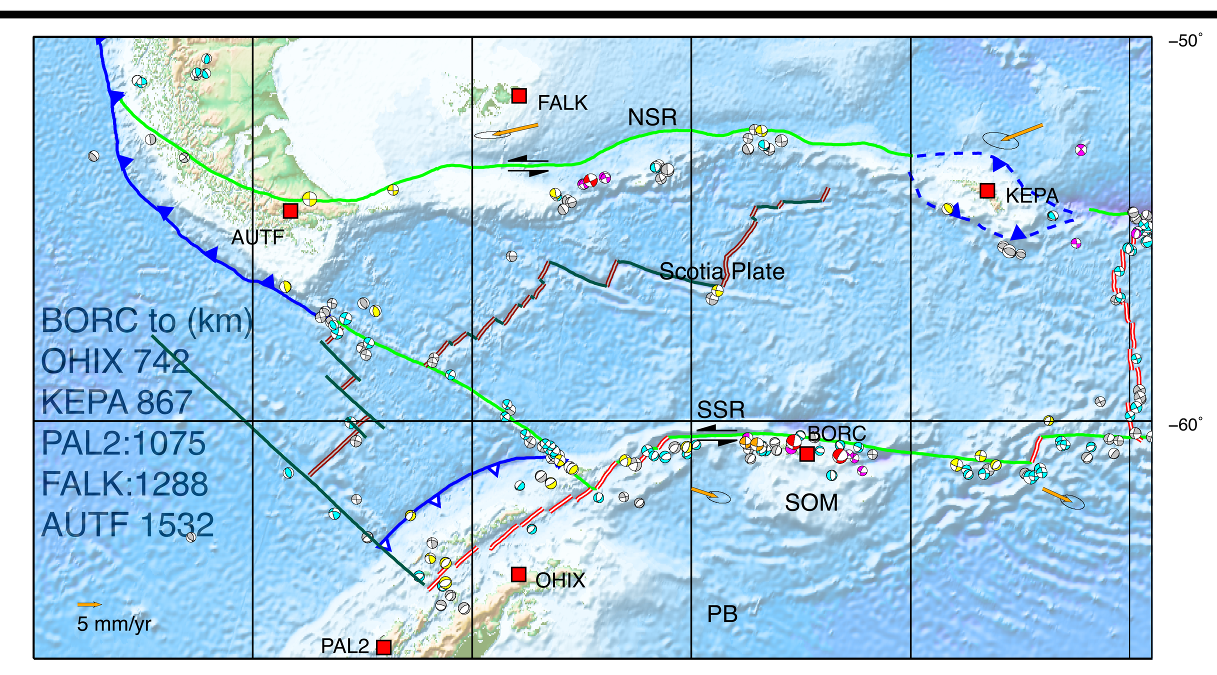

Fig 2. Scotia plate seismotectonics. Plate boundaries; green - transform; double red - active spreading centers; blue - subduction, barbs on upper plate, active - filled, inactive - open, extinct boundaries in darker colors, dashed lines indicate inferred. Focal mechanisms for larger earthquakes along SP margins. Red: mainshocks (Mw 7.8, 11/17/2013 [western], Mw 7.6, 8/4/2003 [eastern], both on SSR near BORC, and a possibly triggered Mw 7, 11/25/2013 on North Scotia ridge), orange: immediate foreshocks 2013 (Mw 6.8, 11/16/2013, Mw 6.1, 11/13/2013), gray: earthquakes before 2003, cyan: between 2003 and 2013, magenta: aftershocks 2013 SSR event, from GCMT. Yellow: Pelayo and Wiens (1989), and Alvarado (unpublished). South America and Antarctic relative plate motions with respect to SP shown by orange vectors.

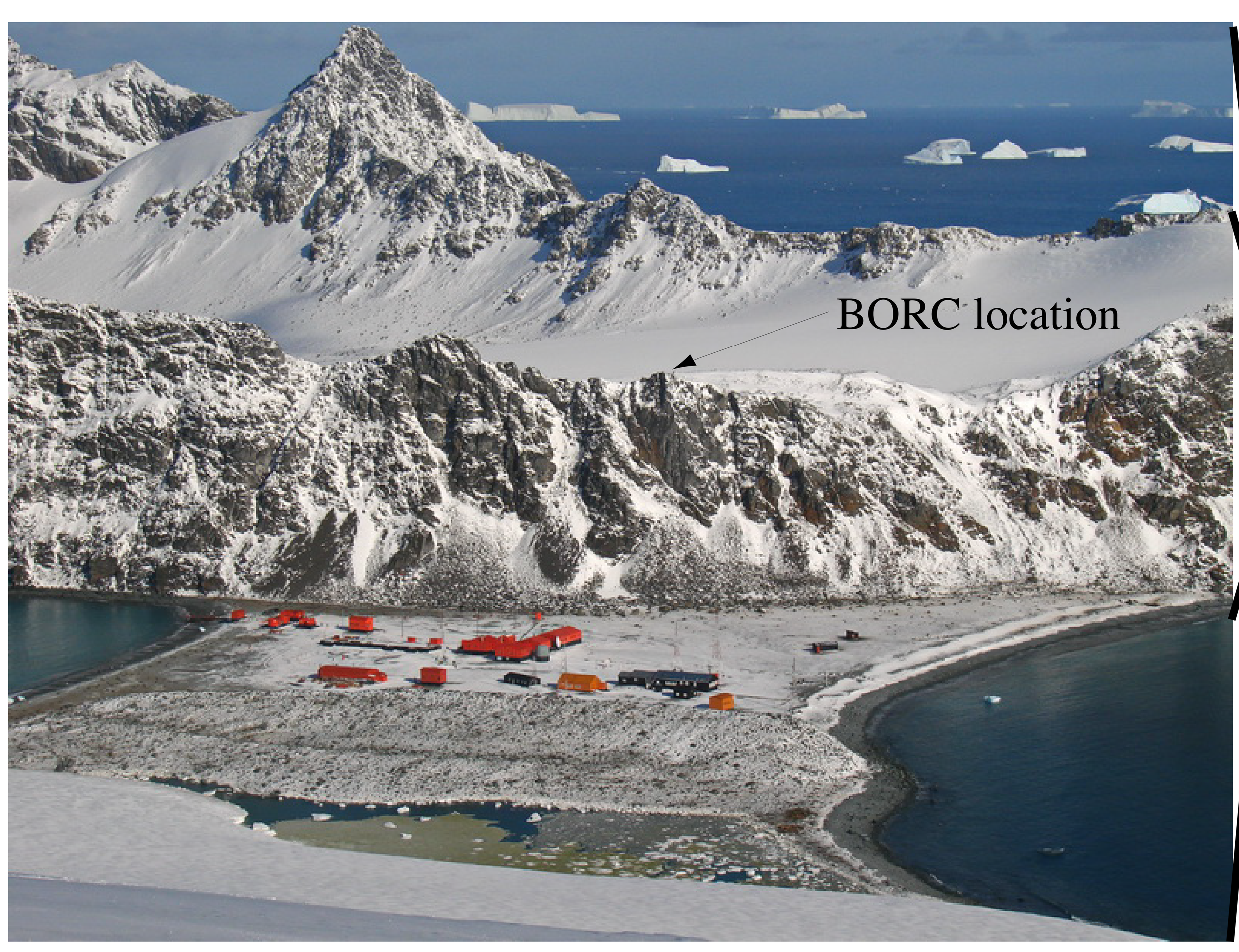

Fig 3. Argentine base on Laurie Island, South Orkney Islands. It is the oldest, continuously operating Antarctic base. It was founded in 1903 (giving the 2003 earthquake its name, the "centennial" earthquake) by the Scottish National Antarctic Expedition and transferred to Argentina in 1904. On-site operation and maintenance of the CGPS station BORC has been performed by Park Rangers from the Argentine National Parks since installation in 1999.

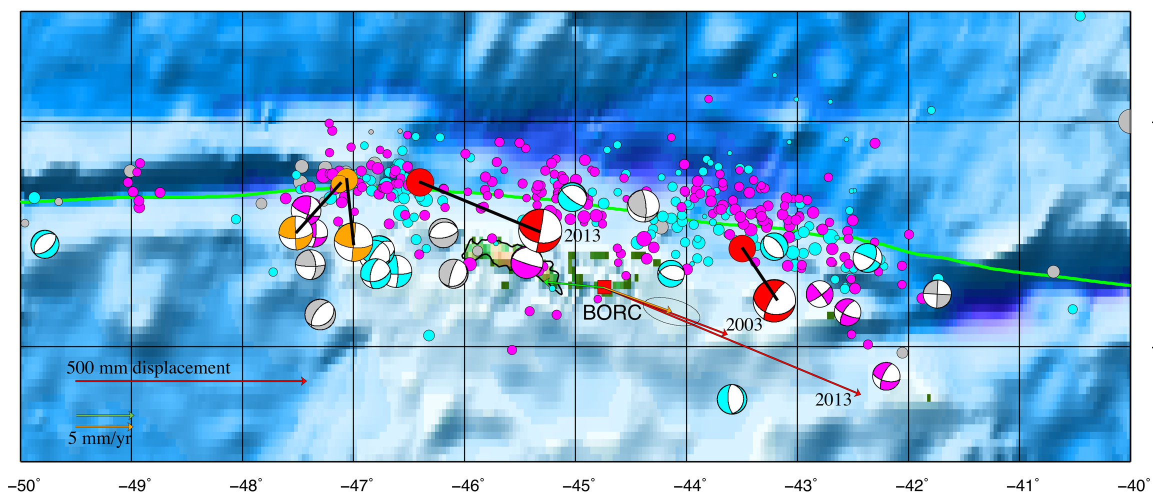

Fig 4. Seismotectonics. Coseismic static displacements (red vectors) for 2003 and 2013 events at CGPS station BORC. BORC interseismic velocity vectors with respect to SP (orange) and AP (green). BORC is located on the AP and in the plate boundary deformation zone. BORC inter- and co-seismic motions are consistent with predominantly S-S tectonics. BORC coseismic displacements are approximately opposite interseismic motion and ~100 times larger, consistent with a seismic cycle of hundreds of years. Note different scales for interseismic velocities and coseismic displacements. Main shocks (beachballs at GCMT locations with line to PDE location), colors as in Fig 2. A seemingly shared fault between two large events on the same segment of plate boundary 10 years apart was challenging to explain in elastic rebound/seismic gap models, but the aftershock distributions are complementary. Ye et al. (2014), using global seismic data and the GPS seismograms and static offsets presented here, show the two events did not rupture the same fault plane.

The mainshocks also occurred on shallow dipping (30-45°), ~EW oriented faults with almost pure (2013), or largely (2003), S-S motion (in both the CMT and geodetic solutions), an unusual, and unstable geometry for S-S faults. Fault geometry is thought to be tectonically inherited from SOM's original position near the tip of the AP (Fig 2), or acquired as it moved to its current location. Strain and slip partitioning usually develop vertical S-S faults over the down-dip fault edge in such geometries. Juxtaposition of continental/stretched continental crust against oceanic crust may play a role in maintaining this ususual geometry. While BORC is ~100 km from the epicenter, as rupture progressed eastward for >200 km the rupture's downdip edge passed approximately beneath BORC due to the southward shallow dip of the fault plane.

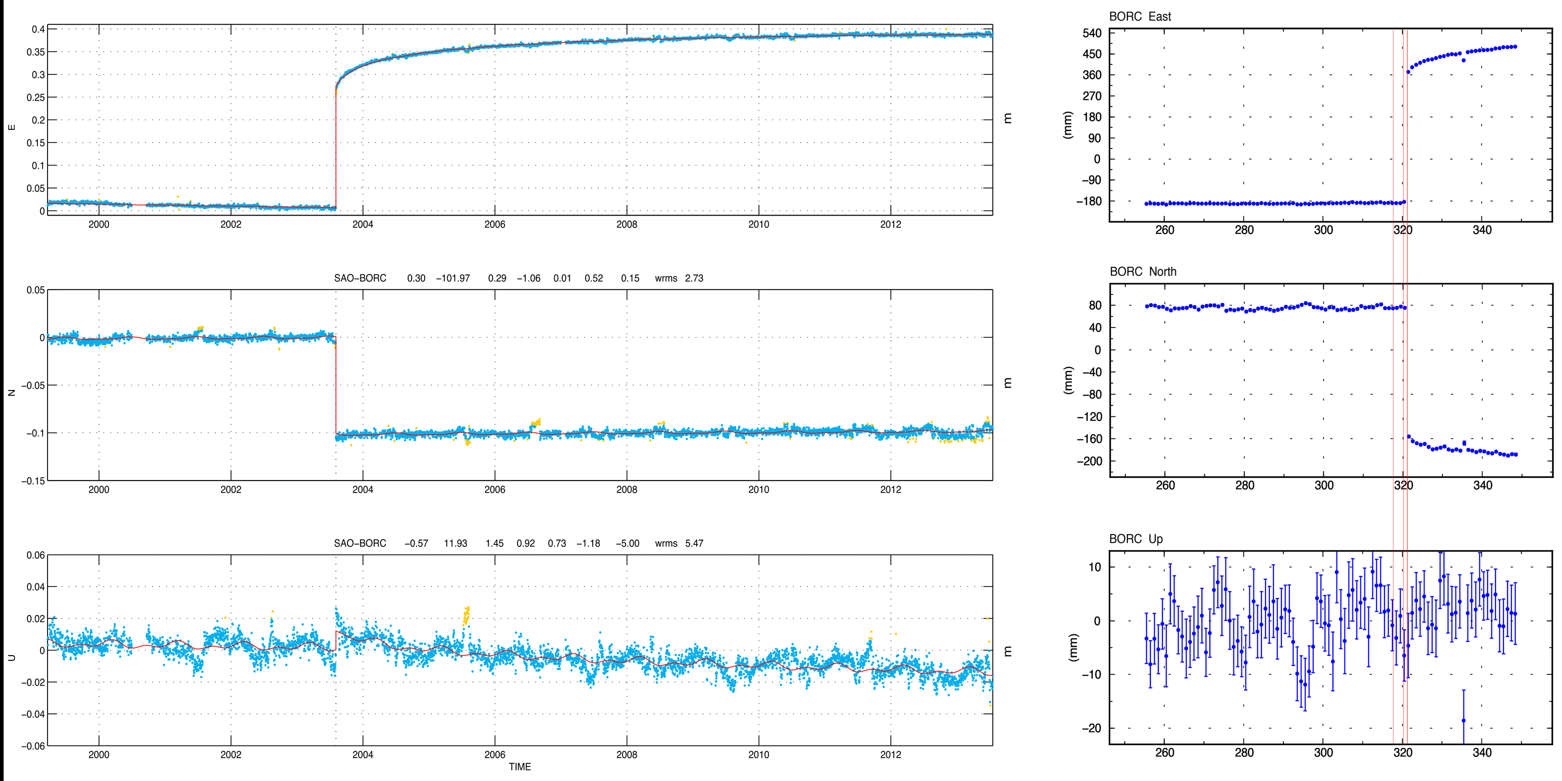

Fig 5. GPS displacement time series for BORC, located ~40 km south of bathymetric morphological expression of plate boundary. Left, time series showing coseismic displacements for 2003 event (NEU in meters: -0.102, 0.269, 0.012), with an unexpectedly long postseismic response (Bevis and Brown, 2013). Right, time series showing coseismic and intial postseismic response of 2013 event. There was no observable vertical offset associated with the 2013 event. Red vertical line on right indicates day of the 2013 mainshock (NEU in meters: -0.232 , 0.557, 0 within errors, total 0.603 m), thin red lines indicate foreshocks. There is no discernable coseismic offset for the first and a hint of EW coseismic offset for the second. The small vertical coseismic offset associated with the 2003 event seems to separate a period of no vertical movement from one with a slow decrease in height for which we have no clear explanation (isostatic adjustment, dynamic topography?). Note: coseismic displacements are estimated from an average of pre-event daily positions, and the average position the day after the event. We used the last 15 hours of the day of the earthquake to estimate post event position for the 2013 event, so there are no "missing" days). Using "daily" positions, coseismic displacement estimates will always be too large as they include the initial, most rapid part, of the postseismic displacements.

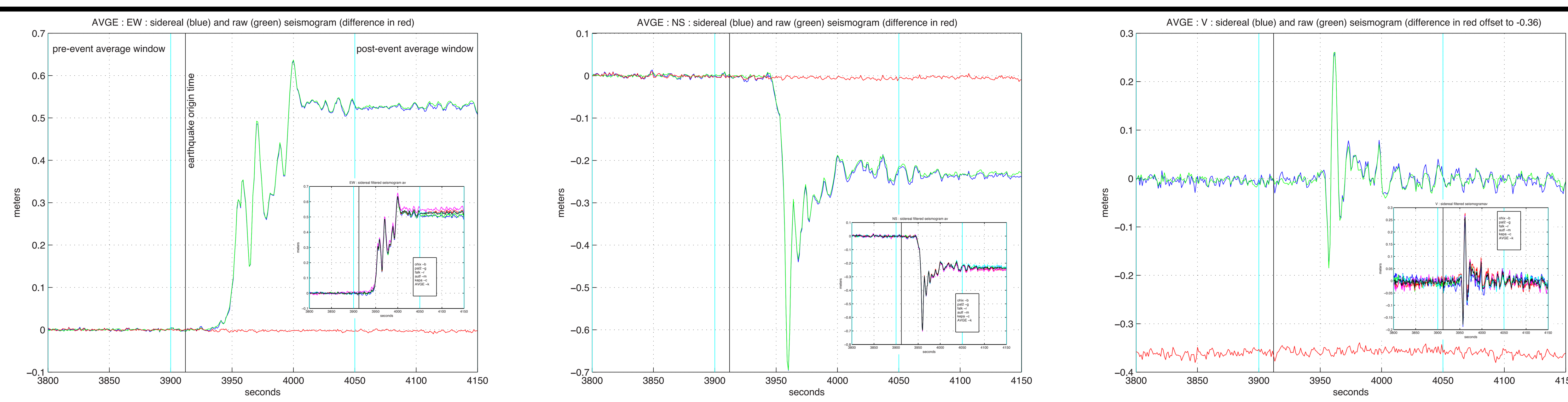

Fig 6. High-rate (1 Hz) GPS displacement seismograms at BORC for Mw 7.8, Nov 17, 2013, SSR earthquake estimated using TRACK (Herring, 2009). Raw (green) and sidereally filtered (blue) seismograms, and difference (red). TRACK calculates differential per-epoch baselines that are transformed to local NEU at one end (BORC end selected). We used all 1 Hz continuous GPS stations within 1600 km of BORC (see Fig 2) processing individual station pairs (BORC to each, shown in the insets) and use the average. The UD (vertical) time series contained large, linear drifts that have been removed. The individual estimations, are in very good agreement among themselves. Pre- and post-event average positions are calculated in the windows indentified on the EW plot. The pre-event average is removed and static coseismic displacement is estimated - NEU in meters: -0.235, 0.525, 0.005, total horizontal 0.575. This is smaller than that estimated from Fig 5 by 0.003 and 0.032 m in NS and EW respectively, for 0.032 m total, a difference of ~5%. In addition to errors related to the estimations, the static offset in Fig. 5 also has additional displacement due to post seismic deformation, visible in the daily time series. In the first two full days after the event the EW and NS displacements increased by 0.022 and -0.011 m respectively. The GAMIT post event position on the day of the earthquake was estimated using the 15 hour period remaining after the earthquake. This position estimate includes both coseismic offset, that occurred over ~100 seconds (a relatively long duration for an M7.8 earthquake), and a rapid postseismic component that may be as large as 0.01-0.02 m during the remainder of the day and could fully account for the difference in coseismic displacemet estimates.

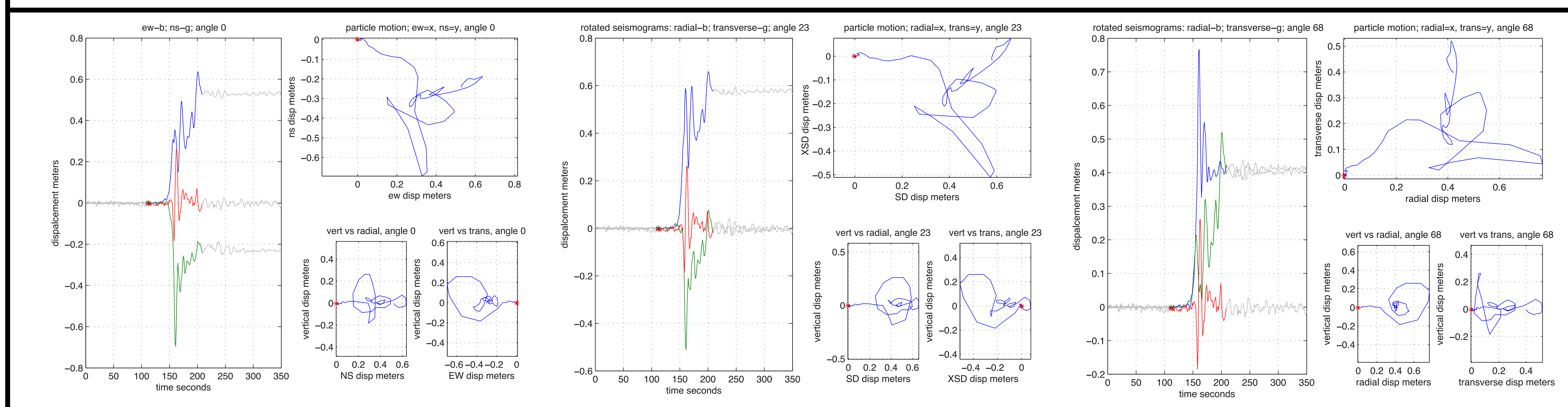

Figure 8. Particle motion (PM) analysis of GPS displacement seismograms. The left set of panels shows unrotated NS time series in green, EW in blue and UD in red. In the two sets of rotated panels, blue is the static displacement (SD, center) or radial (right), and green is the cross static displacment (XSD, center) or transverse (right). The top right plot of each set, with the horizontal components, simply rotates from one set to the next. Red asterisks show start time for the particle motion plots. Horizontal PM is relatively well separated in time and polarized. The center set of panels is a rotation (23° ccw) into the coseismic static displacement direction (SD). The right set of panels shows the rotation (68° ccw) producing the cleanest separation into Rayleigh (radial) that arrive first, which is unusual, and Love (transverse), wave motions. The particle motion plots show the oftentimes observed "overshoot" of the displacement in the near field, that in this case can be explained as the passage of the surface waves and is not a dynamic overshoot and subsequent return of the slip/displacement on the fault. The modeling of Ye et al., 2014, show this more rigorously.

Bevis, M., A. Brown, Trajectory models and reference frames for crustal motion geodesy, J. Geodesy, 2014, 88, 3, 283-311, doi: 10.1007/s00190-013-0685-5.

Civile, D., E. Lodolo, A. Vuan, M.F. Loreto, Tectonics of the Scotia-Antarctica plate boundary constrained from seismic and seismological data, Tectonophysics, 2012, 550–553, 17–34, doi: 10.1016/j.tecto.2012.05.002.

Dalziel, I. W. D., L. A. Lawver, I. O. Norton, and L. M. Gahagan, The Scotia Arc: Genesis, evolution, global significance, Ann. Rev. Earth Planet. Sci., 41, 767-793, 2013, doi:10.1146/annurev-earth-050212-124155.

Herring T.A., .TRACK GPS kinematic positioning program, version 1.21. Massachusetts Institute of Technology, Cambridge, 2009.

Lingling Ye, Thorne Lay, Keith D. Koper, Robert Smalley Jr., Luis Rivera, Michael G. Bevis, Andrés F. Zakrajsek, Felix Norman Teferle, Complementary slip distributions of the August 4, 2003 Mw 7.6 and November 17, 2013 Mw 7.8 South Scotia Ridge earthquakes, Earth and Planetary Science Letters, Volume 401, 1 2014, 215-226, doi:10.1016/j.epsl.2014.06.007.